Analytical Methods

Accepted Manuscript

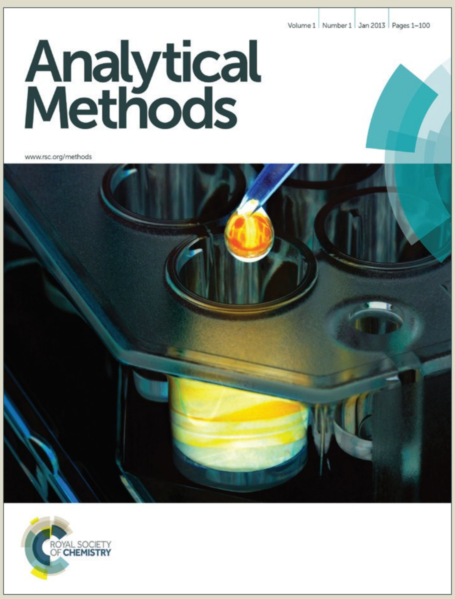

Investigation of CdO hexagonal nanoflakes synthesized by hydrothermal method for liquefied petroleum gas detection

Weijun Xia[a,b] Yanli Liu[a,b]* Junhua Li[a,b] Chao Chen[a,b]

[a] College of Material Science and Engineering, Hunan University, Changsha 410082, China

[b] Hunan Province Key Laboratory for Spray Deposition Technology and Application, Hunan University, Changsha 410082, China

*Corresponding Author: Yanli Liu, Email: yanliliu@hnu.edu.cn

Tel: 86-731-8882 1610; Fax: 86-731-8882 1610

Address: College of Materials Science and Engineering, Hunan University, Changsha 410082, China

Abstract: Cadmium oxide (CdO) hexagonal nanoflakes demonstrated clearly in SEM image were synthesized via a one-step hydrothermal method. The formation of CdO was confirmed by XRD spectra and EDS spectra taken from CdO nanoflakes. To demonstrate the potential applications, gas sensor was fabricated and gas sensing test showed that the sensor exhibited significantly high response to liquefied petroleum gas (LPG) and short response/recovery time. The enhancement of sensing performance was attributed to the unique structure and greater number of surface active sites on the surface of as-prepared gas-sensing material, which provided the increased contact surface area between CdO and gas analytes.

Keywords: Hexagonal nanoflake; CdO; Hydrothermal method; Gas sensor

1. Introduction

In recent decades, conductometric gas sensors based on metal oxides have been widely investigated for the detection of toxic pollutant gases, combustible gases, and organic vapors [1-4]. It is widely accepted that surface oxygen species could trap electrons from the conduction band of metal oxides and the subsequent reaction between adsorbed oxygen and the test gases would bring about a resistance change. [5]. The aggregation of the nanomaterials with regular morphology, such as nanospheres, is still serious, which reduces the remained space for gas diffusion inside the metal oxide sensing layer. It is difficult for the tested gas molecules diffusing into the interior of the sensing layer, resulting in a poor utilization rate of the sensing materials located in the internal location [6]. The preparation of sensing materials with a specific structure, which can remarkably improve the gas-diffusing properties in gas sensor, has been considered to be a fascinating approach to address the problems indicated above. Many nanomaterials with special structures have been achieved, such as nanotudes, flower-like nanostructures, etc [7-9]. It was reported that the response, response/recovery speed could be improved by these structures [10].

Cadmium oxide (CdO) is a known n-type semiconductor with outstanding catalytic, optical, and electrical properties enabling its application in various scientific and industrial fields [11-15]. As a promising candidate for gas sensor, CdO has a high carrier mobility and high conductivity (10^3 Ω^{-1} cm^{-1}) due to the presence of oxygen vacancies leading to a non-stoichiometric composition [16, 17]. In the present work, CdO nanoflakes prepared by a simple hydrothermal route without any post-synthesis annealing treatment were reported. In gas-sensing measurements, LPG (liquefied petroleum gas) was employed as a target gas. It was found that the as-prepared nanosturctures exhibited a remarkably gas responses toward analytes as well as fast response and recovery speeds.

2. Experimental

2.1 Materials Synthesis

All of the reagents were analytical purity and were used without further purification. Deionized water was used throughout the experiments. In a typical synthesis, extra potassium hydroxide (KOH, 20 g) was added to 10 mL of cadmium nitrate tetrahydrate aqueous solution ($Cd(NO_3)_2 \bullet 4H_2O$, 0.2 mol/L) at room temperature with vigorous agitation. And the mixture was stirred for another 2 h before being transferred into a Teflon-lined stainless steel autoclave that was subsequently sealed and heated to 260 °C and maintained for 24 h. The mixture had been cooled to room temperature naturally after the reaction, the resulting precipitate was collected by centrifugation and washed several times with ethanol and deionized water alternately and dried at 70 °C in air for further characterization.

For comparison, CdO nanospheres were prepared by the precipitation method. 10 ml of 0.4 mol/L KOH aqueous solution was added to 10 mL of cadmium nitrate tetrahydrate aqueous solution (0.2 mol/L) drop by drop with vigorous agitation. The mixture was kept at room temperature for another 4 h with slow stirring before the product was collected by centrifugation. The product was then washed with deionized water and absolute ethanol, and dried at 70 °C in air. The final products were obtained after calcinations at 400 °C in air for 2 h.

2.2 Materials Characterizations.

X-ray powder diffraction (XRD) patterns were obtained on the Rigaku D/Max-2000 instrument using Cu Kα radiation (λ = 0.15418 nm). The morphology of the products were studied by field emission scanning electron microscopy (FESEM, Hitachi S-4800) in conjunction with energy-dispersive X-ray (EDS) measurements, transmission electron microscopy (TEM; Tecnai F20) and high-resolution transmission electron microscopy (HRTEM; Tecnai F20) at an accelerating voltage of 200 kV, respectively. UV-vis diffuse reflection spectra (UV-vis DRS) were recorded on UV-vis spectrometer (U-4100, Hitachi) in the range of 300-800 nm. Here, $BaSO_4$ was used as the reflectance standard material.

2.3 Fabrication of the Gas Sensor and Gas-sensing Detection

Firstly, a proper amount of the paste consisting of CdO obtained and absolute ethanol was dropping on alumina ceramic tubes mounted with two Au electrodes. Secondly, after the evaporation of ethanol, a small Ni-Cr wire was placed through the tube as a heater. The operating temperature of the gas sensors was controlled by adjusting the current flow applied on the heater. Thirdly, electrical contacts were made with two Pt wires attached to each Au electrode and the sensors were aged under working conditions for 48 h in order to enhance the signal stability. WS-30A static gas-sensing system (Weisheng Electronics Co. Ltd., Henan, China) was used to examine the performance of the sensors. The response of the sensors was studied in a test chamber (18 dm^3) with a gas inlet and an outlet. The gas analytes was injected into the test chamber through the gas inlet and the voltage was measured as a function of time till it attained constant value. Then the chamber was purged with fresh air and the experiments were repeated. All gas-sensing detections were performed at the relative humidity values, 20% RH.

3. Results and Discussion

Fig. 1 shows the XRD patterns of CdO nanostructures. Fig. 1a and Fig. 1b represent CdO nanoparticles and CdO nanoflakes, respectively. The peaks assigned as (111), (200), (220), (311) and (222) plane are of cubic structures of CdO (JCPDS card No. 05-0640). Moreover, the absence of other diffraction peaks adequately demonstrates the high purity of synthesized composites without any by-products formed. The morphology of the final products was investigated and shown in Fig. 2. The presence of hexagonal nanoflakes is clearly demonstrated in SEM image (Fig. 2a). Furthermore, it can be seen that there exhibits strong peaks of Cd, and O peaks in the EDS spectra taken from CdO nanoflakes (Fig. 2b), which confirms the formation of CdO. The edge length of the CdO flakes is about 100 nm and the thickness is about 45 nm as shown in TEM image (Fig. 2d). The HRTEM image is shown in the inset of Fig. 2d and the interplanar distances of fringes are measured to be 0.27 nm, which correspond to the spacing of the (111) plane of CdO. In contrast, CdO nanospheres with a smooth surface prepared by precipitation method are shown in Fig. 2c and the particle sizes are differed.

The UV-vis absorption spectra of CdO are presented in Fig. 3a. It is obvious to see a sharp basal absorption edge for CdO. The band gap energy of CdO is estimated based on the well-established equation: $\alpha = A(hv - E_g)^{1/2} / hv$, where α, E_g, and A are the absorption coefficient, band-gap energy, and constant, respectively (shown in Fig. 3b) [18]. By extrapolating the linear region in the plots of $(\alpha hv)^2$ versus hv, the E_g of CdO is about 2.25 eV.

In gas-sensing measurements, LPG (liquefied petroleum gas) is employed as a target gas. The response of gas sensors is defined as the ratio of resistance in the air (Ra) to that in the gas analytes (Rg): S=Ra/Rg. Fig. 4a shows the response of the sensor based on CdO nanoflakes as a function of working temperature of CdO sensor upon exposure to 500 ppm of LPG. The sensor based on CdO nanoflakes exhibits its optimal response at the working temperature, 270 ^{o}C. At lower working temperatures, the sensor response is restricted by the speed of the chemical reaction between the adsorbed oxygen and LPG, and at higher temperatures it is restricted by the speed of diffusion of LPG [19, 20]. At some intermediate temperature, the speed values of the two processes become equilibrium, and the sensor response reaches its maximum.

The real-time sensing curve of the sensor based on CdO nanoflakes to detect 500 ppm of LPG is shown in Fig. 4b. It is obvious that the resistance decreases with the time and then remains constant when LPG is injected into the detecting chamber. When fresh air is introduced, the resistance increases again. The LPG-sensing mechanism of the sensor may be explained as follows. CdO in its pure form belongs to n-type semiconducting sensor materials due to oxygen vacancies and interstitial cadmium atoms that act as donors. The adsorption of atmospheric oxygen on the semiconductor surface can trap electrons from the conduction band of semiconductor to form ionic species such as O_2^- and O^- [21-23]. The equilibration of the chemisorptions process results in stabilization of surface resistance (measured as *Ra*). The oxygen adsorption reactions may be expressed by the following chemical equations [24, 25]:

$O_2(g) \rightarrow O_2(ads)$

$O_2(ads) + e^- \rightarrow O_2^-(ads)$

$O_2^-(ads) + e^- \rightarrow O_2^{2-}(ads)$

$O_2^{2-}(ads) \rightarrow 2O^-(ads)$

Wherein ‘g’ and ‘ads’ refer respectively to gas and adsorbate.

When CdO is exposed to the atmosphere containing LPG, the reaction between adsorbed oxygen and LPG would release the captured electrons back to the conduction band and the overall resistance of the sensor drops (measured as *Rg*). It is well known that LPG consists of CH_4, C_3H_8, C_4H_{10}, etc [26]. The overall reaction of LPG molecules with adsorbed oxygen species may be illustrated as follows:

$C_nH_{2n+2}+O^-(ads)\rightarrow CO_2+H_2O+e^-$

Here C_nH_{2n+2} represents the CH_4, C_3H_8 and C_4H_{10}.

When fresh air is introduced again, CO_2 and water vapor could be removed out from the semiconductor and again oxygen is chemisorbed. The resistance of the semiconductor increases again.

The response and recovery time are defined as the time taken by the sensor to achieve 90% of the total resistance change in the case of adsorption and desorption, respectively. The response time and recovery time are observed to be about 8.6 s and 10 s, respectively as shown in Fig. 4b. The fast response with quick recovery behavior of the developed sensor could be explained by taking into account the fast LPG diffusion toward the nanoflake surface and its reaction with surface oxygen. LPG diffusion toward the surface of CdO is relatively easier compared to powder samples because of the minor agglomeration between the flakes seen in the SEM image (Fig. 2a). The results here reported are in agreement with the shortening of response time as decreasing the edge size and thickness of SnO_2 sheet previously reported [27].

Fig. 5 presents the dynamic variation of sensor responses as a function of LPG concentrations obtained from CdO nanoflakes and nanoparticles at the working temperature of 270 ^{o}C. As expected, the sensor based on CdO nanoflakes (Fig. 5a) exhibits much higher sensing properties than that of CdO nanoparticles (Fig.5b). The real-time sensing curves increase step by step depending on the elevation of LPG concentrations. It can be supported by the calculated values of response shown in the inset of Fig. 5a and Fig. 5b, respectively. The response amplitude of the sensor is significantly increased with LPG concentration increment. There is no obvious saturated state can be observed, indicating that the presented gas sensor would possess a large detecting range of gas concentration.

4. Conclusion

In summary, the present work reported the synthesis of CdO nanostructures by a simple of hydrothermal route. The sensing characteristics of the devices on the CdO nanostructures were investigated. The developed sensor exhibited high sensing performance to LPG and presented short response/recovery time due to due to less agglomerated structures between the thin CdO flakes. This demonstrated that the present chemical route is a facile way to form high-quality CdO nanostructures to be used as the LPG gas sensor.

Acknowledgement

This work was financially supported by the National Natural Science Foundation of China (No.61404046), the Science and Technology Planning Project of Hunan Province, China (No. 2014GK3093).

References

[1] M. Chen, Z. Wang, D. Han, F. Gu, G. Guo. J. Phys. Chem. C. 115(2011) 12763-12773.

[2] K. Wetchakun, T. Samerjai, N. Tamaekong, C. Liewhiran, C. Siriwong, V. Kruefu, A. Wisitsoraat, A. Tuantranont, S. Phanichphant. Sens. Actuators B 160 (2011) 580-591.

[3] D. Kohl. J. Phys. D Appl. Phys. 34 (2001) R125-R149.

[4] R. Moos, N. Izu, F. Retting, S. Reiβ, W. Shin, I. Matsubara. Sensors 11 (2011) 3439-3465.

[5] S. Nakagomi, M. Kaneko, Y. Kokubun, Sens. Lett. 9 (2011) 35-39.

[6] R. Moos, N. Izu, F. Retting, S. Reiβ, W. Shin, I. Matsubara, Sensors 11 (2011) 3439-3465.

[7] G. Korotcenkov. Mater. Sci. Eng. B 139 (2007) 1-23.

[8] Z. Chen, M. Cao, C. Hu. J. Phys. Chem. C 115 (2011) 5522-5529.

[9] J. Li, H. Fan, X. Jia. J. Phys. Chem. 114 (2010) 14684-14691.

[10] X. Fu, J. Liu, T. Han, X. Zhang, F. Meng, J. Liu. Sens. Actuators B 184 (2013) 260-267.

[11] N. Rajesh, J.C. Kannan, S.G. Leonardi, G. Neri, T. Krishnakumar, J. Alloys Comp. 607 (2014) 54-60.

[12] B. Saha, S. Das, K.K. Chattopadhyay, Sol. Energy Mater. Sol. Cells 91 (2007) 1692-1697.

[13] F. Yakuphanoglu, M. Caglar, Y. Caglar, S. Ilican, J. Alloys Comp. 506 (2010) 188-193.

[14] X. Liu, C. Li, S. Han, J. Han, C. Zhou, Appl. Phys. Lett. 82 (2003) 1950-1952.

[15] R.K. Gupta, K. Ghosh, R. Patel, P.K. Kahol, J. Alloys Comp. 509 (2011) 4146-4149.

[16] D.M.C. Galicia, R. C. Perez, O. J. Sandoval, S. J. Sandoval, G. T. Delgado, C.I. Z. Romero, Thin Solid Films 371 (2000) 105-108.

[17] D. S. Raja, T. Krishnakumarb, R. Jayaprakasha, T. Prakasha, G. Leonardic, G. Neri, Sens. Actuators B 171-172 (2012) 853-859.

[18] M. A.Butler, J. Appl. Phys., 48 (1977) 1914-1920.

[19] R.J. Deokate, C.D. Lokhande. Sens. Actuators B 193 (2014) 89 -94.

[20] S. Bai, L.Chen, D. Li, W. Yang, P. Yang, Z. Liu, A. Chen, C.L. Chung. Sens. Actuators B 146 (2010) 129-137.

[21] Q. Wan, Q. H. Li, Y. J. Chen, T. H. Wang, X. L. He, J. P. Li, C. L. Lin, Appl. Phys. Lett. 84 (2011) 3654-3656.

[22] N.K. Singh, S. Shrivastava, S. Rath, S. Annapoorni. Appl. Surf. Sci. 257 (2010) 1544-1549.

[23] J. Xu, X. Jia, X. Lou, J. Shen, Solid-State Electron. 50 (2006) 504-507.

[24] C.S. Prajapati, S.N. Pandey, P.P. Sahay, Phusica B 406 (2011) 2684-2688.

[25] P.P. Sahay, S. Tewari, S. Jha, M. Shamsuddin, J. Mater. Sci. 40 (2005) 4791-4793.

[26] L.A. Patil, D.N. Suryawanshi, I.G. Pathan, D.M. Patil, Sens. Actuators B 176 (2013) 514-521.

[27] C.S. Moon, H. R. Kim, G. Auchterlonie, J. Drennan, J. H. Lee, Sens. Actuators B 131 (2008) 556-564.

Figure Captions:

Fig. 1. XRD patterns of CdO: (a) CdO nanoparticles; (b) CdO hexagonal nanoflakes.

Fig. 2. (a) SEM image of CdO hexagonal nanoflakes; (b) EDS spectra taken from CdO nanoflakes; (c) CdO nanospheres prepared by precipitation method; (d) TEM image of CdO hexagonal nanoflakes. Inset: HRTEM of CdO hexagonal nanoflakes.

Fig. 3. (a) UV-vis diffuse reflectance spectroscopy of CdO hexagonal nanoflakes; (b) plots of $(\alpha h\nu)^2$ vs. photo energy ($h\nu$) of CdO.

Fig. 4. (a) Sensor response *vs.* working temperature of gas sensor based on CdO hexagonal nanoflakes; (b) Dynamic response-recovery curve of to 500 ppm of LPG at working temperature of 270 ^{o}C.

Fig. 5. Dynamical response curves of CdO sensor to 10 to 2000 ppm of LPG at working temperature of 270 ^{o}C; Inset: The calibration curve of the sensor to LPG with increasing concentrations: (a) Gas sensor based on CdO hexagonal nanoflakes; (b) Gas sensor based on CdO nanospheres.

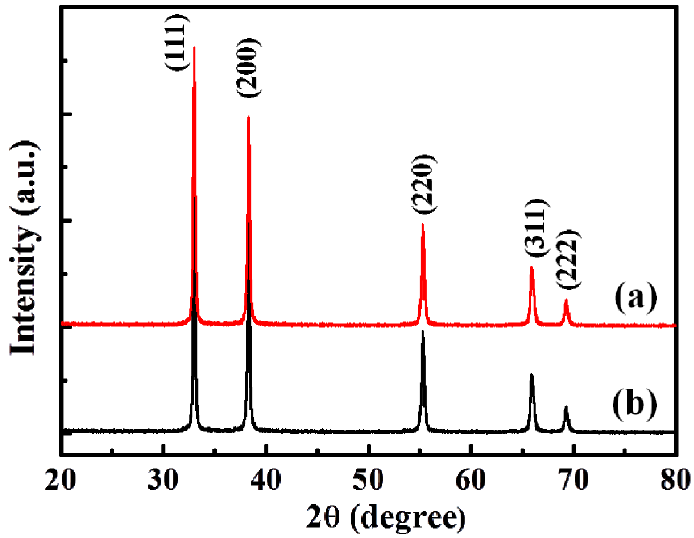
(111)
(200)
(220)
(311)
(222)
(a)
(b)
Intensity (a.u.)
20
30
40
50
60
70
80
2θ (degree)

Fig. 1

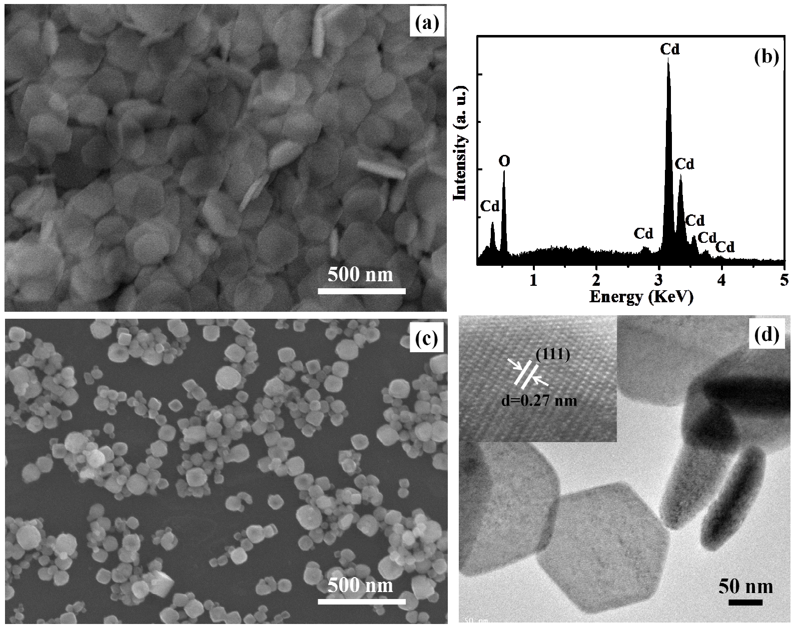
(a)
500 nm
(b)
Cd
O
Cd
Cd
Cd
Cd
Cd
Cd
Intensity (a. u.)
Energy (KeV)
1
2
3
4
5
(c)
500 nm
(d)
(111)
d=0.27 nm
50 nm

Fig. 2

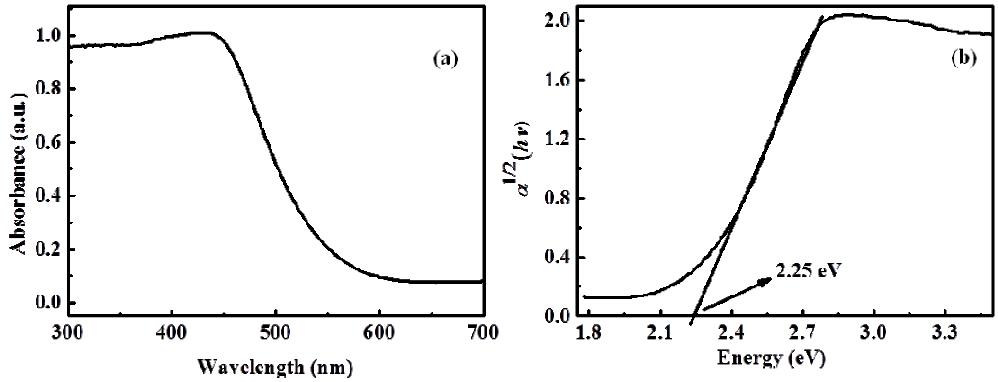

Fig. 3

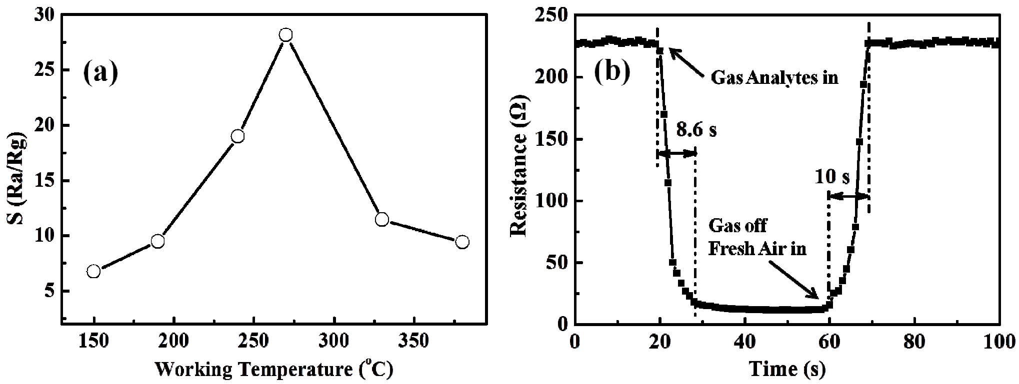

(a)
S (Ra/Rg)
Working Temperature (°C)
30
25
20
15
10
5
150
200
250
300
350
(b)
Resistance (Ω)
Time (s)
Gas Analytes in
8.6 s
10 s
Gas off
Fresh Air in
250
200
150
100
50
0
20
40
60
80
100

Fig. 4

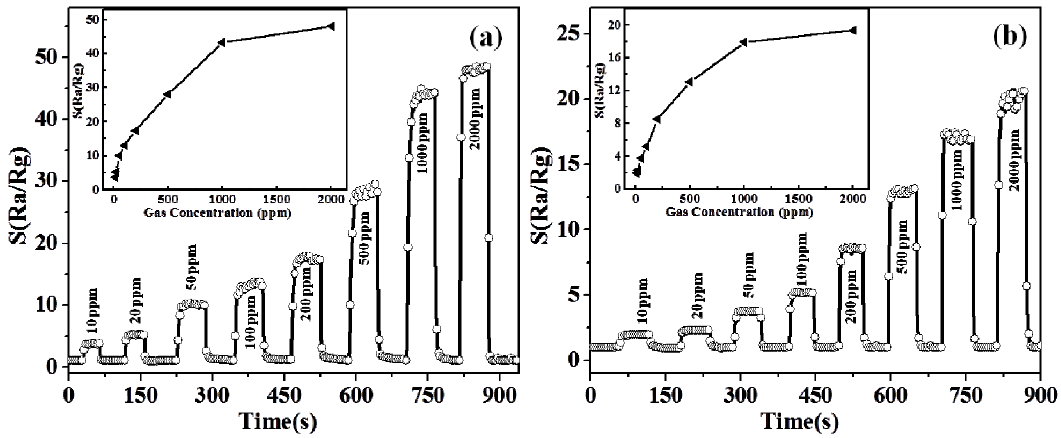
(a)
(b)
S(Ra/Rg)
Time(s)
Gas Concentration (ppm)
10ppm
20ppm
50ppm
100ppm
200ppm
500ppm
1000ppm
2000ppm

Fig. 5